



# Subsurface thermal structure: a climate science perspective

Félix García Pereira<sup>1,2</sup>, J. F. González Rouco<sup>1,2</sup>, N. Steinert<sup>1,2</sup>, and C. Melo Aguilar<sup>1,2</sup>

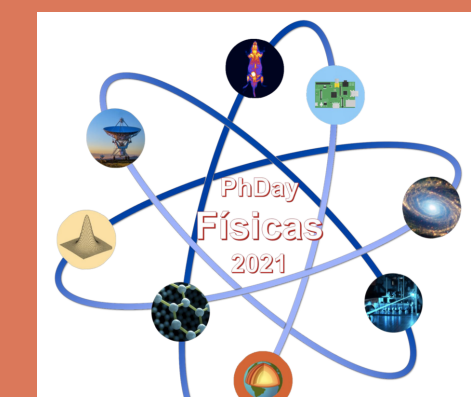
<sup>1</sup>Universidad Complutense de Madrid, Facultad de Ciencias Físicas, Departamento de Física de la Tierra y Astrofísica

<sup>2</sup>Instituto de Geociencias, IGEO (UCM-CSIC)



Corresponding author: Félix García Pereira

felgar03@ucm.es



## Abstract

Land-atmosphere interaction occurs at a wide range of time scales in the form of mass, momentum, and energy exchange (Melo-Aguilar et al., 2018). Further, subsurface holds a water and mostly energy storehouse for the climate system, accounting for around a 6 % of the terrestrial energy storage (Cuesta-Valero et al., 2021). Therefore, determining the subsurface thermal structure is key to understanding its influence on the global energy balance and hydrological cycle. This work explores the nature of the subsurface thermal regime both in models and in observations.

The Max Planck Institute Earth System Model (MPI-ESM) is considered and the sensitivity of its subsurface thermal regime analyzed to changes of the model depth, this being a limitation in the current generation of climate models. It is found that such changes have important implications for the evolution of subsurface temperatures and energy storage in climate change simulations. Additionally, monitoring of subsurface temperatures at some sites allows for estimating thermal diffusivity and seeking causes for its variability in time and space. Results indicate that changes in soil moisture are responsible for the bulk of spatial and temporal variability in apparent thermal diffusivity. The approach developed herein shows a large potential compared to standard approximations focused on the annual cycle.

## 2. Heat conduction in Land Surface Models (LSM)

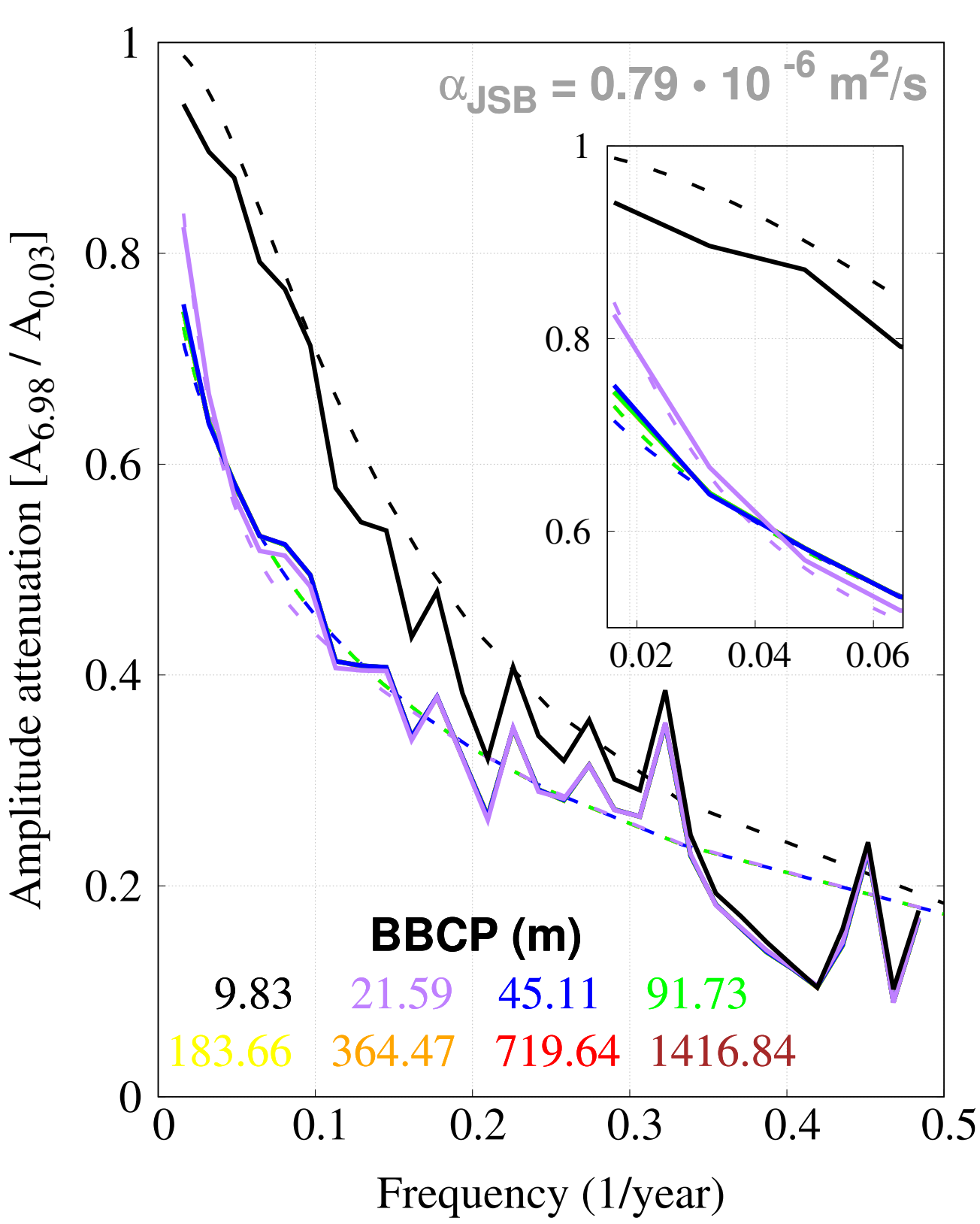
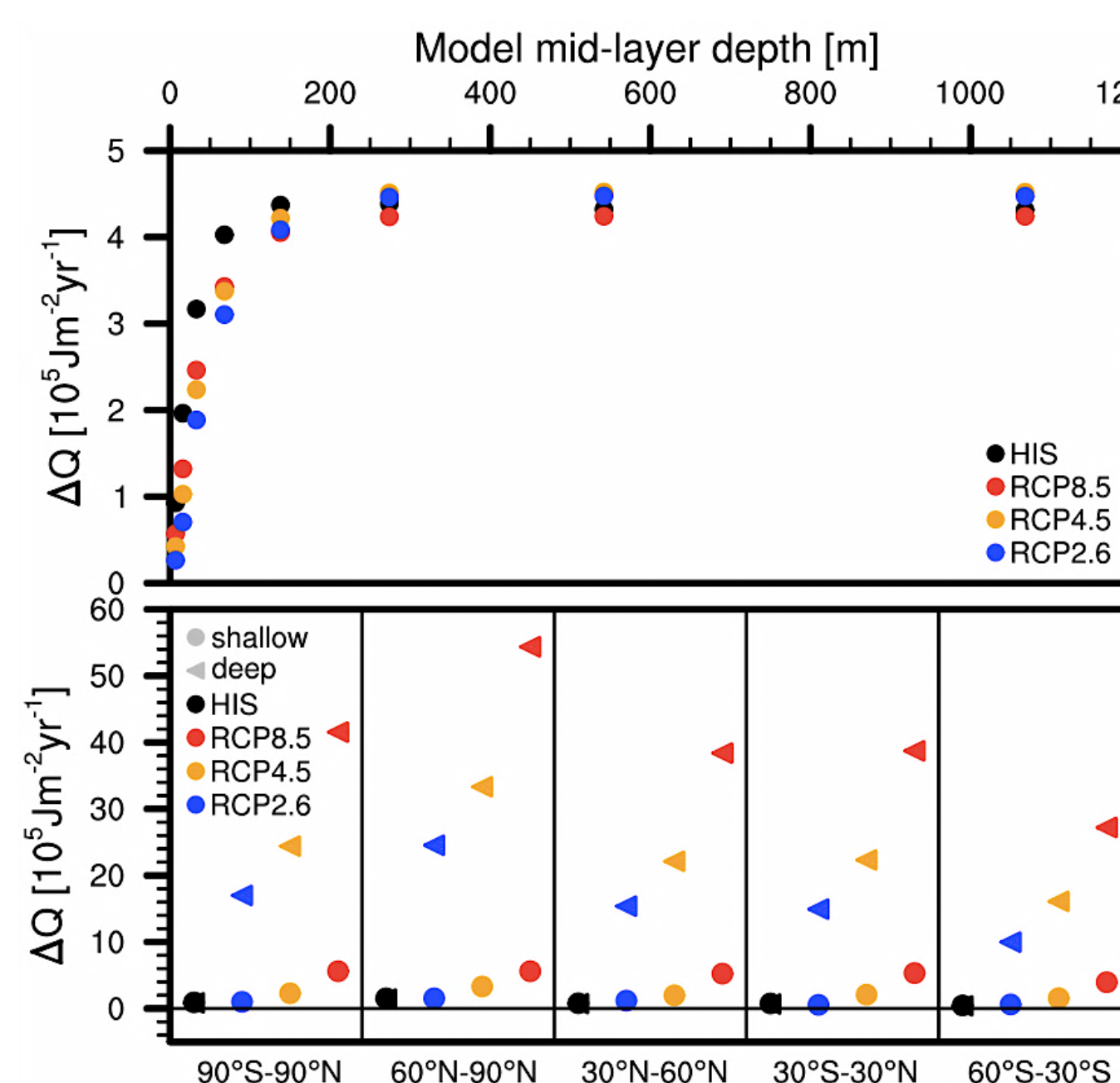


Fig. 3. Spectral amplitude attenuation curves between subsurface temperatures at two levels, 0.03 and 6.98 m, for different BBCP depths. Dashed lines represent the analytical solution, whilst solid lines are derived from global mean yearly averaged subsurface temperature simulated data coming from JSBACH, the land component of MPI-ESM (González-Rouco et al., 2021). Attenuation values at the low frequencies are zoomed in the inset.



Further, they underestimate the heat storage capacity of subsurface by up to 8 times in the RCP8.5 (Fig. 4; González-Rouco et al., 2021). BBCP should be imposed at least at 170 m to avoid attenuation bias (Steinert et al., 2021).

Fig. 4. Heat energy storage assessment in historical and RCP scenario JSBACH standalone simulations. From González-Rouco et al. (2021).

The analysis presented herein shows that:

- a) Climate models must include realistic representations of the subsurface as an infinite half-space with sufficiently large depths to represent well climate change responses.
- b) A new method allows for deducing effective time and space estimates of thermal diffusivity with potential for improving model simulations and deriving reconstructions of (the otherwise scarce) soil moisture variability.

## CONCLUSIONS

García-Pereira, F., J. F. González-Rouco, C. Melo-Aguilar, T. Schmidt, C. Vegas-Cañas, N. J. Steinert: "An assessment of thermal diffusion regime in the subsurface at some sites in Sierra de Guadarrama". In preparation.  
González-Rouco, J. F., N. J. Steinert, E. García-Bustamante, S. Hagemann, P. de Vreese, J. H. Jungclaus, S. J. Lorenz, C. Melo-Aguilar, F. García-Pereira, and J. Navarro: "Increasing the depth of a Land Surface Model. Part I: Impacts on the soil thermal regime and energy storage". Journal of Hydrometeorology (in press), 2021.  
Melo-Aguilar, C., J. F. González-Rouco, N. J. Steinert, H. Beltrami, F. J. Cuesta-Valero, A. García-García, F. García-Pereira, E. García-Bustamante, P. J. Roldán-Gómez, T. Schmidt, and J. Navarro: "Near-surface soil thermal regime and land-air temperature coupling: a case study over Spain". International Journal of Climatology (in revision), 2021.  
Steinert N. J., J. F. González-Rouco, C. Melo Aguilar, F. García-Pereira, E. García-Bustamante, P. de Vreese, V. Alexeev, J. H. Jungclaus, S. J. Lorenz, and S. Hagemann: "Agreement of analytical and simulation-based estimates of the required land depth in climate models". Geophysical Research Letters, 48, e2021GL094273, DOI: 10.1029/2021GL094273, 2021.  
Vegas Cañas C., J. F. González-Rouco, J. Navarro-Montesinos, E. García-Bustamante, E. Rodríguez-Camino, A. Chazara-Bernabé, and I. Álvarez-Arévalo: "An Assessment of Observed and Simulated Temperature Variability in the Sierra de Guadarrama". Atmosphere, 11(9), 985. DOI: 10.3390/atmos11090985, 2020.

## 1. Heat transfer in the subsurface

Heat propagation into the subsurface occurs mainly by conduction, so that ground surface temperature ( $T$ ) changes penetrate into depth following the heat conduction law [1]. The solution for an infinite-half space (Carslaw and Jaeger, 1959) is [2]:

Temperature perturbations are exponentially attenuated and

$$T(z, t) = \bar{T} + \sum_i A_i(0) e^{-z\sqrt{\frac{\pi f_i}{\alpha}}} \cdot \cos(2\pi f_i t + \phi_i(0) - z\sqrt{\frac{\pi f_i}{\alpha}}) \quad [2]$$

linearly phase-shifted with depth ( $z$ ), depending on the harmonic frequency ( $f$ ) and thermal diffusivity ( $\alpha$ ). Figure 1 shows that very clearly for daily and annual signals in ground surface temperatures (GST) at an observational site. The diurnal cycle is completely filtered out in the first soil meter, whilst the annual cycle is hardly perceptible at 15 m. Figure 2 shows the dependence of attenuation on timescale and  $\alpha$ . Signals penetrate deeper for longer timescales and higher diffusivity values.

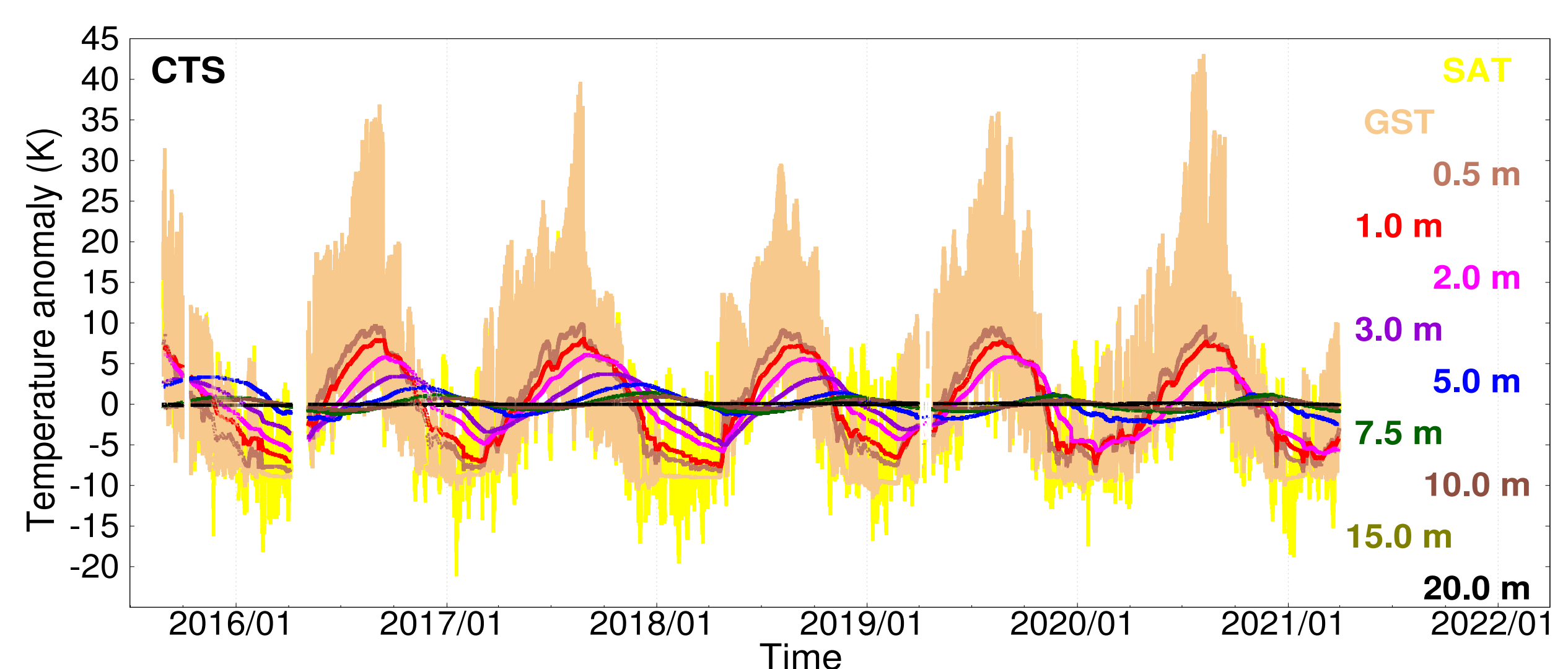


Fig. 1. Subsurface temperature series for various depths at Cotos (CTS; Vegas et al. 2020). Source: GUMLNet (scan QR in red).

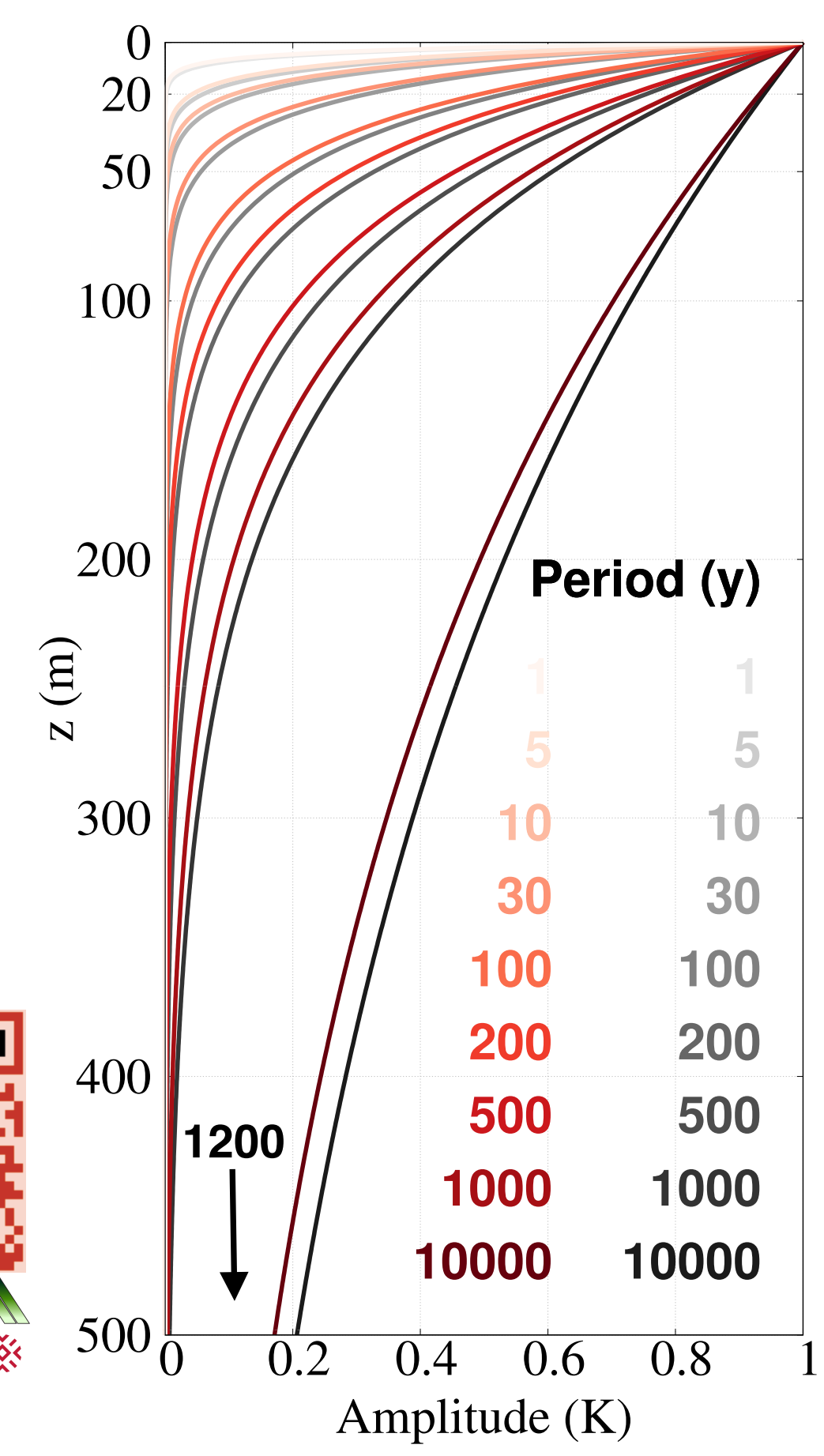


Fig. 2. Attenuation with depth of waves of various frequencies and 1K of amplitude at the ground surface. Values in red (grey) correspond to a constant diffusivity value of  $0.8 \cdot 10^{-6} \text{ m}^2/\text{s}$ . Adapted from Pollack and Huang (2000).

## 3. Real-life subsurface thermal structure

Subsurface heat conduction in observations complies with the infinite-half space solution (see Fig. 1). Apparent heat diffusivity values can be determined by a classical analytical approach, assessing amplitude attenuation and phase shift of the annual wave with depth (CAA; Fig. 5; Smerdon et al. 2004). An application of the CAA method to time series in the Iberian Peninsula shows spatial variability in apparent diffusivity that follows the spatial distribution of soil moisture (Fig. 6).

However, the latter method requires several years of observations at various depths to perform a good fit of the parameters in Eq. [2] and derive  $\alpha$ . This hampers the assessment of temporal variability. A new spectral attenuation-based method (SAM; García-Pereira et al., 2021) allows for retrieving the apparent diffusivity value of shorter time series by focusing on the attenuation at all frequencies (e.g. Fig. 7). The application of SAM to the time series of subsurface temperatures in Fig. 1 allows for estimating the high-frequency changes of  $\alpha$ . See an example for 10-daily estimates in Fig. 7. Apparent diffusivity follows observed soil moisture changes in time.

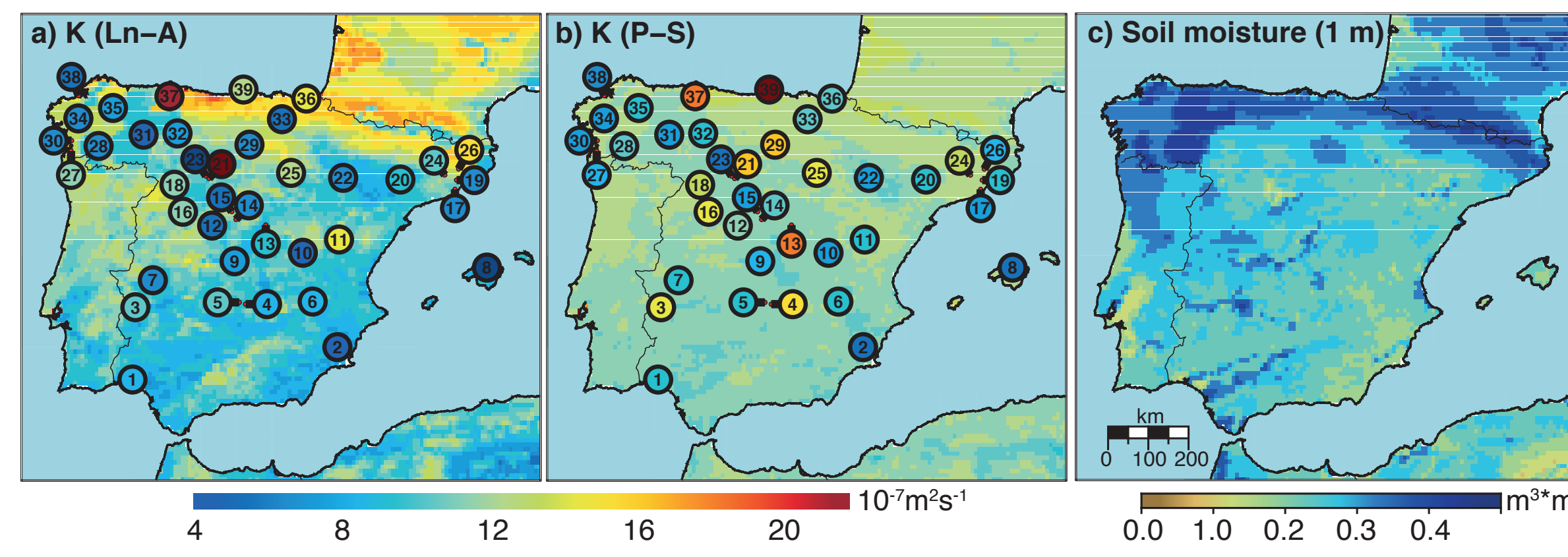


Fig. 5. CAA applied to Cotos (CTS) and Hoyas (HYS). Data in depth are integrated from different sources (see legend) down to 20 m.

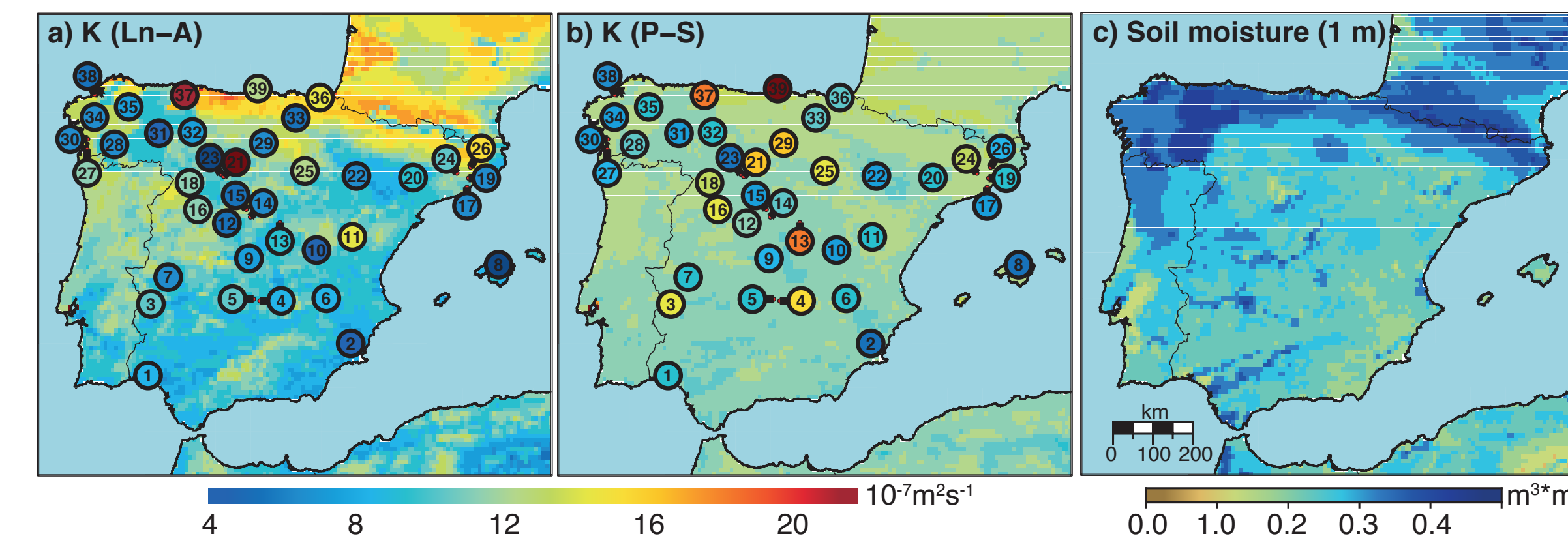


Fig. 6. Apparent diffusivity derived from CAA (a,b) and integrated soil moisture content (c) for some observational (circles) and ERA-Interim reanalysis subsurface temperatures down to 1 m in the Iberian Peninsula (Melo-Aguilar et al., 2021).

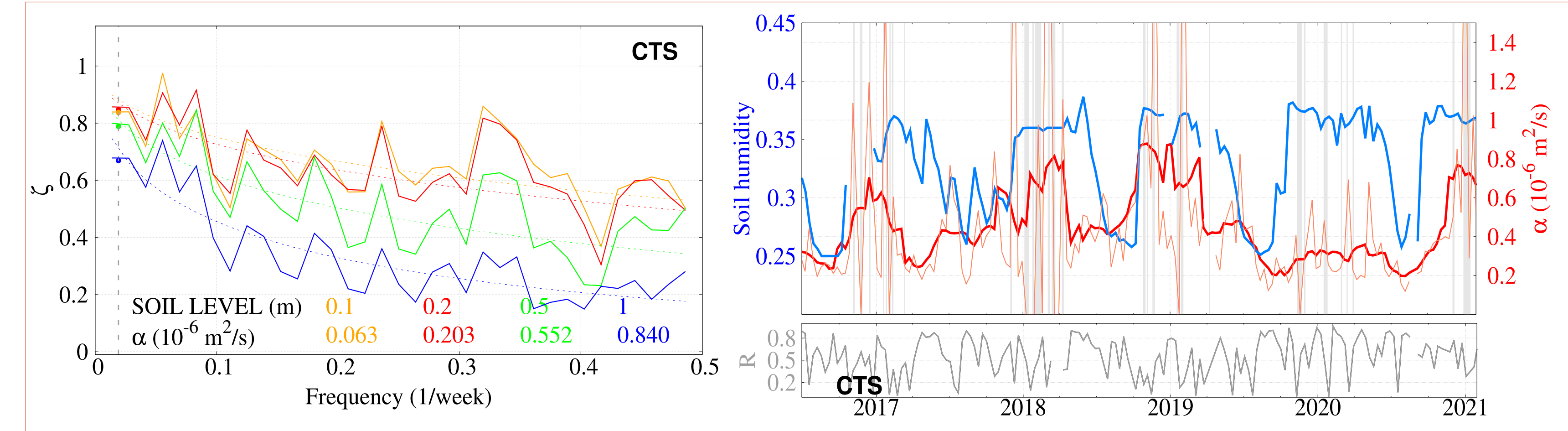


Fig. 7. (Left) SAM applied to CTS shallow subsurface temperature series in weekly resolution. (Upper right) Soil humidity (blue) and apparent diffusivity (red) at CTS from mid-2017 to 2021 in 10-daily resolution. Soil apparent diffusivity was calculated performing SAM in a 240-hourly-data running window. (Lower right) Goodness-of-fit of SAM.